

Microcirculatory Changes in Livers of Mice Infected with Murine Hepatitis Virus. Evidence from Microcorrosion Casts and Measurements of Red Cell Velocity

P. J. MACPHEE,* E. E. SCHMIDT,† P. A. KEOWN,*‡ AND A. C. GROOM†

*Departments of Medical Biophysics, *Microbiology and Immunology, and †Medicine, Health Sciences Centre, University of Western Ontario, London, Ontario, Canada N6A 5C1

Received March 17, 1988

Hepatitis has been considered, classically, as a diffuse hepatocellular necrosis, and little attention has been paid to the relationship of lesions to the microvasculature. In livers of mice (Balbc/J) infected with murine hepatitis virus (MHV-3), microcorrosion casts showed spherical cavities where casting compound was unable to fill sinusoids. At 48 hr postinfection such "lesions" had a mean diameter of $83 \mu\text{m} \pm 26$ (SD) and their number/mm² (at the surface of casts) was 0.95 ± 1.3 . Blind-ended sinusoids formed a distinct boundary between perfused and nonperfused areas, and concave impressions at their ends indicated cells blocking the lumen. *In vivo* microscopy of transilluminated livers in infected mice showed localized rounded areas without flow, corresponding to lesions seen in casts. RBC velocity measurements in sinusoids adjacent to lesions demonstrated that velocities fall from normal values to zero over a narrow border zone. Beginning with the most proximal sinusoid with visible flow and moving outward from the lesion to the second and third sinusoids, mean RBC velocities ($\mu\text{m/sec.} \pm \text{SD}$) were 17.4 ± 6.7 , 33.9 ± 8.7 , 66.6 ± 27.3 , respectively; this last value was not significantly different from velocities in normal liver (69.2 ± 30.6). Transmission electron microscopy of livers of infected mice confirmed the presence of sinusoidal lumens blocked by protruding lining cells, RBCs, platelets, swollen hepatocytes, and cellular debris. This study demonstrates that the lesions are focal in origin, microvascular blockage leading to gradually increasing necrosis in all directions. © 1988 Academic Press, Inc.

The classical view of hepatitis is that of a diffuse hepatocellular necrosis, and very little attention has been paid to the relationship of the lesions to the microvasculature. The model that has been employed to investigate this relationship uses murine hepatitis virus type 3 (MHV-3) infection of susceptible (Balbc/J), semisusceptible (C3HeBFe/J), and fully resistant (A/J) strains of mice, which parallels the various possible human responses to hepatitis viruses. It has been suggested that MHV-3 may have a direct cytopathic effect on hepatocytes (Le Provost *et al.*, 1975), but no mechanism has yet been proposed to explain the early flow changes observed in the microcirculatory bed. Thus, in susceptible mice discrete regions of decreased blood flow in the hepatic sinusoids appear as early as 12–24 hr postinfection (Levy *et al.*, 1983); rounded localized areas without flow, adjacent to terminal portal venules, can be distinguished even at low magnifications. Comparison of *in vivo* microcirculatory views with histological sections (light microscopy) (Levy *et al.*, 1983; MacPhee *et al.*, 1985) revealed

that these flow changes occurred before areas of recognizable cellular necrosis were seen. In contrast, in the fully resistant (A/J) mice no microcirculatory changes were seen following infection, despite the presence of high titers of replicating virus.

The purpose of the present investigation was to study the microcirculatory changes in livers of mice infected with MHV-3, and to explore the following questions: Is there red blood cell (RBC) flow through the lesions themselves? How does RBC flow change as a function of distance from the periphery of the lesion? Are the lesions uniform in size, and how are they distributed? What insights can be gained from these findings regarding the mechanisms of initiation and spread of the lesions? The primary methods employed were scanning electron microscopy (SEM) of microcorrosion casts, and *in vivo* microscopy of the trans-illuminated liver, in both infected and control mice.

MATERIALS AND METHODS

Balbc/J mice, 5 weeks old, were obtained from Jackson Laboratories, Bar Harbor, Maine, and were used at 6–10 weeks of age. MHV-3 was obtained from the American Type Culture Collection, Rockville, MD (ATTCC VR 262), and stock cultures were grown in L cells.

Microcorrosion casts: In preparation for corrosion casting of the liver, the abdominal aorta was cannulated and heparin (50 USP/100 g body wt) was administered to prevent clotting. The body was perfused with Ringer's solution at 100 cm H₂O pressure for 20 min or until the liver was blanched, the vena cava having been cut for drainage. At this time a modified, low viscosity Batson's casting compound (Nopanitaya *et al.*, 1979) was injected manually via the arterial cannula. The liver was left undisturbed for 1.5 hr during polymerization; it was then cut into several pieces and the tissue digested in 40% KOH at 60° for 3–4 days. The cast was then rinsed in distilled H₂O, air-dried, mounted on SEM stubs, and sputter-coated with gold. The casts were examined using a Philips 501 scanning electron microscope. Size and frequency data regarding lesions were obtained from low-power photomicrographs.

In vivo microscopy. Mice were injected with MHV-3 (10,000 PFU ip) and examined at 24–48 hr postinfection (p.i.). Anesthesia was induced with sodium pentobarbital, 6 mg/100 g body wt. A midline abdominal incision was made and the mouse was placed on its side on the platform of an inverted microscope, so that one lobe of the liver lay on a window positioned over the objective lens. The liver was moistened continuously by a saline drip (37°), and the animal's rectal temperature was monitored and maintained at 37° with a heat lamp. The liver was covered with Saran wrap which held it gently against the coverslip window, restricting lateral and vertical motion (due to respiration and heart beat) at the plane of focus. Illumination was provided by a Volpi HL250 fiber-optic light source, positioned obliquely relative to the liver, which resulted in improved image contrast. Objective lenses ranging in power from 10 to 100× (oil immersion) were used. A Panasonic video camera (WV-1550, Newvicon tube with extended red sensitivity) was mounted in the inverted microscope and the image was displayed on an Electrohome monitor. A Panasonic WJ-810 character generator added stopwatch information to the videosignal, which was recorded using a

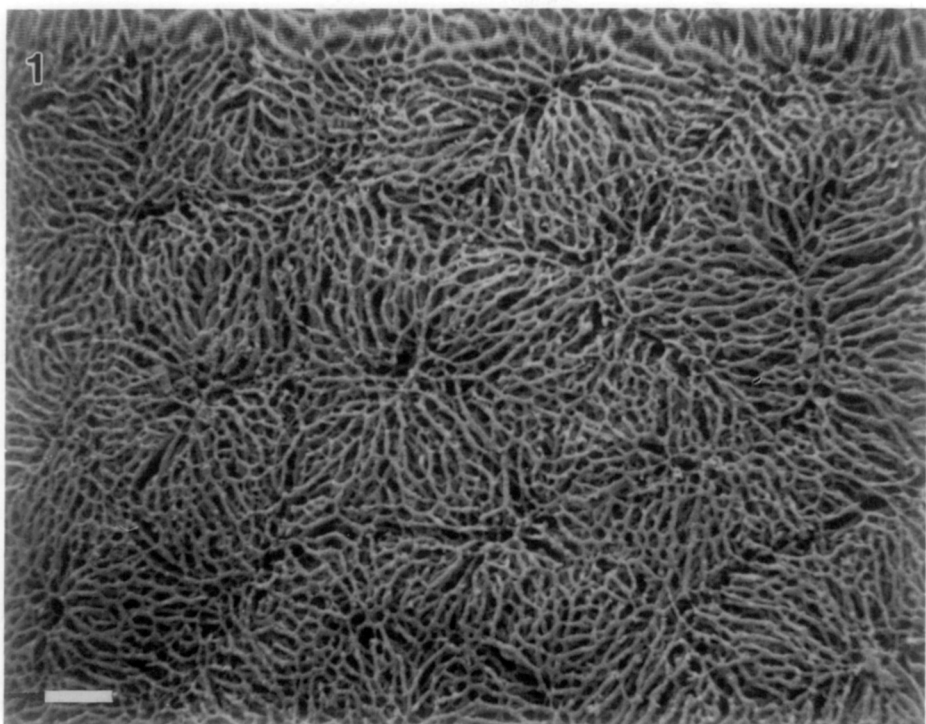


FIG. 1. Microcorrosion cast of normal mouse liver showing complete filling of surface sinusoids in a normal acinar arrangement. Bar = 100 μm ; $\times 90$.

Panasonic NV-9240XD videocassette recorder. This technique has been described in detail recently (MacDonald *et al.*, 1987).

RBC velocities in liver sinusoids were measured from video recordings, using the flying spot method (Tym and Ellis, 1982). Briefly, the recordings were made at a magnification such that individual RBCs could be distinguished clearly. Later, the tape was played back at reduced speed (usually 1/5) and the sweep frequency of a spot traversing the video screen was adjusted such that the velocity of the spot matched that of RBCs moving along a particular sinusoid. The computed velocity of the spot was shown on a digital readout.

Transmission electron microscopy. Liver tissue was fixed by immersion in 2.5% glutaraldehyde in 0.1 M sodium cacodylate buffer for a minimum of 24 hr at 4°, followed by postfixation in 1% osmium tetroxide for 45 min. The tissue was block-stained with uranyl nitrate and lead acetate, dehydrated through graded concentrations of alcohol to acetone, and embedded in Epon. Thin sections were viewed using a Zeiss 109 microscope.

RESULTS

The surface of corrosion casts from liver of normal mice showed complete filling of sinusoids in a normal acinar arrangement (Fig. 1). In casts from infected mice lesions were found having the appearance of approximately spherical cavities, indicating where the casting compound was unable to fill the sinusoids (Fig. 2).

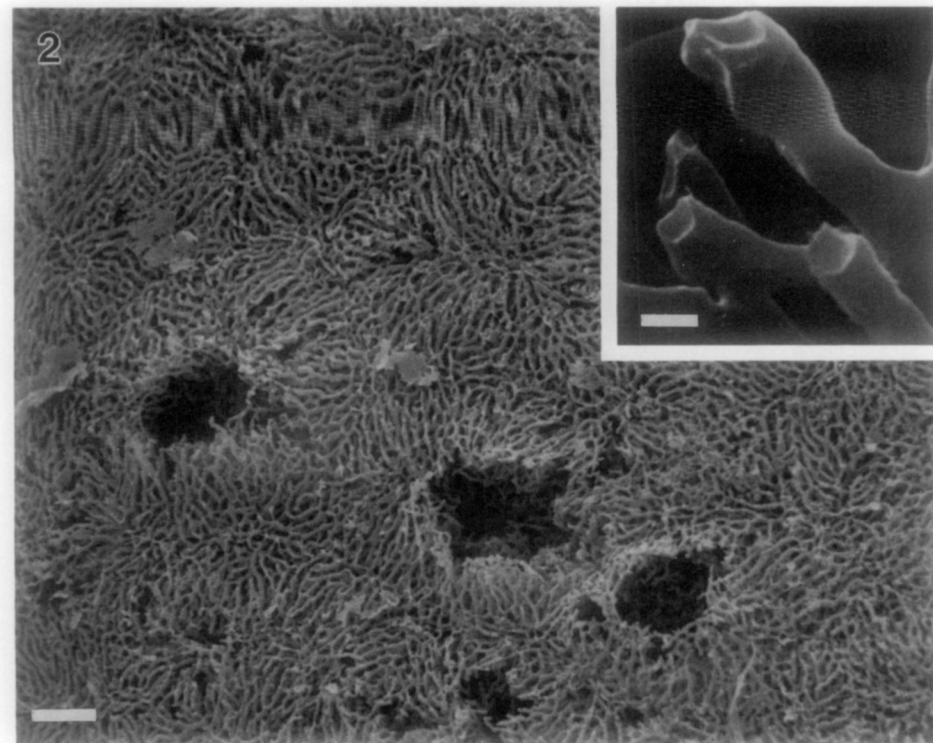


FIG. 2. Microcorrosion cast of liver from MHV-3 infected mouse (48 hr postinfection). Localized areas without filling represent sites of lesions. Bar = 100 μm ; $\times 86$. Inset: High magnification view of "blind-ended" sinusoids at the boundary of a lesion. Note concave impressions at blind ends of sinusoids, caused by blood cells which blocked the lumen. Bar = 5 μm ; $\times 1500$.

The size and distribution of the lesions was determined by measuring these discrete areas from photomicrographs of the casts. At 48 hr post infection the mean diameter was $83 \pm 26 \mu\text{m}$ ($n = 110$), with a range of 44–178 μm . The number of lesions/ mm^2 ranged from 0.2 to 4.3, with a mean value of 0.95 ± 1.3 (SD). This value of 1 lesion/ mm^2 corresponds to about 1 lesion per liver acinus (the area supplied by one terminal portal venule). Views of microcorrosion casts of individual lesions, obtained at higher magnification (Fig. 3), show many "blind-ended" sinusoids forming a distinct boundary between the perfused and nonperfused areas. At still higher magnification many of these sinusoids were seen to have concave impressions at their ends (Fig. 2: inset) as if further passage of the material had been prevented by cells which blocked the lumen. The size of these indentations (5–7 μm) is consistent with that of RBCs.

Transillumination *in vivo* of the liver margin of infected mice showed localized rounded areas without flow, corresponding to the unperfused areas seen in the casts. The pale central zone in Fig. 4 represents the area without flow; in the surrounding sinusoids, which are darker and easily distinguishable because of the presence of RBCs, flow was seen *in vivo*. Velocities of RBCs in liver sinusoids of both normal (Fig. 5) and MHV-3-infected mice were measured from video recordings of flow taken at high magnifications. In infected mice, the RBC velocities were measured in consecutive sinusoids adjacent to and aligned with the periphery

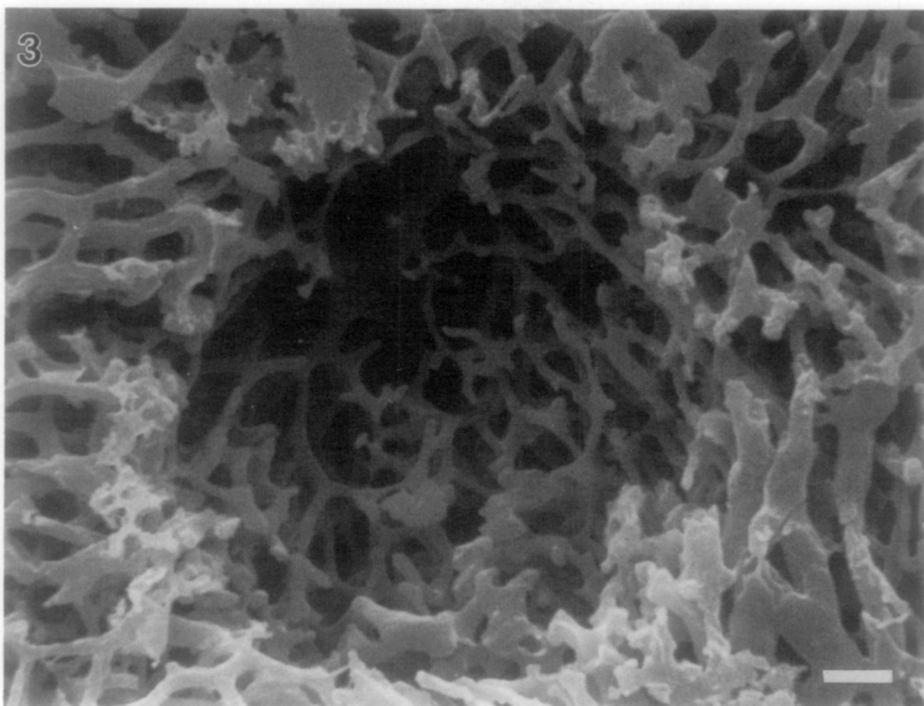


FIG. 3. Microcorrosion cast of liver from MHV-3 infected mouse (48 hr postinfection), showing the distinct boundary between the perfused and nonperfused areas at the site of an individual lesion. Blind ends of sinusoids indicate flow blockage. Bar = 25 μm ; $\times 380$.

of a lesion, beginning with the most proximal sinusoid with visible flow ("first" sinusoid) and moving outward from the lesion. These values are shown in Table 1. The mean velocities in the first and second sinusoids were significantly lower than the mean velocity in normal liver (Student *t* test), whereas the mean velocity in the third sinusoid was not significantly different from normal values. This demonstrates that RBC velocity falls from normal values down to zero over a narrow border zone surrounding the lesion; the width of this zone corresponds to only three sinusoids (i.e., three to six hepatocytes).

TEM of livers of infected mice at 24–48 hr p.i. shows a number of ultrastructural changes affecting sinusoids, sinusoidal lining cells, and hepatocytes. Some sinusoidal lumens appear to be blocked by protruding sinusoidal lining cells, red cells, platelets, swollen microvilli, and cellular debris. In some cases nearby hepatocytes have a pale, vacuolated appearance with indistinct margins bordering on the sinusoids. In Fig. 6, such pale hepatocytes with convex surfaces can be seen bordering a blocked sinusoid; three adjacent sinusoids (S) appear to be patent.

DISCUSSION

The diameters of the lesions at 48 hr postinfection were remarkably uniform, suggesting that the lesions may all have originated at the same time. The mean diameter of 83 μm represents the width of about six hepatocytes and their

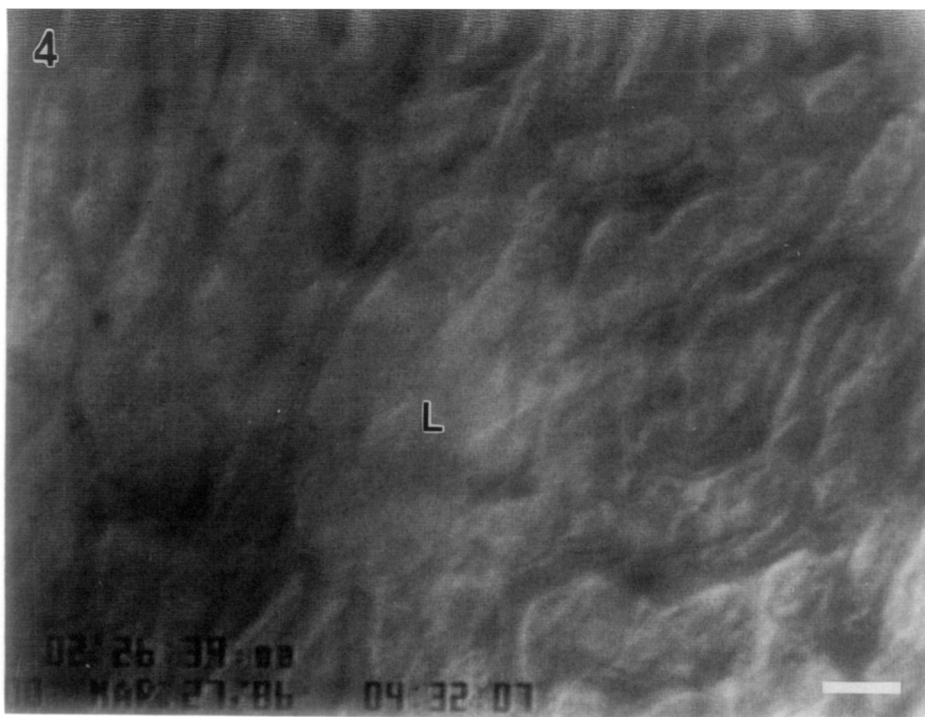


FIG. 4. *In vivo* microscopic view of transilluminated liver margin from MHV-3-infected mouse (48 hr postinfection). In pale central zone no blood flow was seen; this represents site of a lesion (L). In surrounding sinusoids, darker because of presence of RBCs, flow was seen *in vivo*. Bar = 25 μ m; $\times 425$.

sinusoids. Previous *in vivo* microcirculatory studies (Levy *et al.*, 1983) have shown that the lesions enlarge progressively until they reach near confluence at the time of death, 5–7 days postinfection. The low power SEM views of the casts show clearly the highly focal nature of the early lesions caused by the virus (MHV-3). The blind-ended casts of sinusoids at the edges of lesions indicate blockage of the lumens by cells; whether blood cells, sinusoidal lining cells, or swollen hepatocytes are involved cannot be distinguished from the casts.

Video recordings of the microcirculation in livers of infected mice showed normal flow except in focal areas corresponding to the lesions. The transition zone between nonperfused and normally perfused areas was extremely narrow, as shown by measurements of RBC velocity in sinusoids adjacent to the lesions. A previous *in vivo* microscopic study (Bloch *et al.*, 1975) using CF-1 mice infected with MHV-3 also pointed out the focal nature of the lesions, and made the qualitative observation that roughly 20 μ m outside the immediate periphery of the necrotic areas RBC flow appeared normal. These authors commented that *in vivo* microscopy had not been able to shed light on the process by which the hepatic microvascular system in the lesions was destroyed. However, the flow blockage we found was frequently associated with local narrowing of a sinusoid, causing a white cell to plug the lumen, transiently or for prolonged periods. TEM micrographs confirmed the presence of blocked sinusoids, characterized by cells

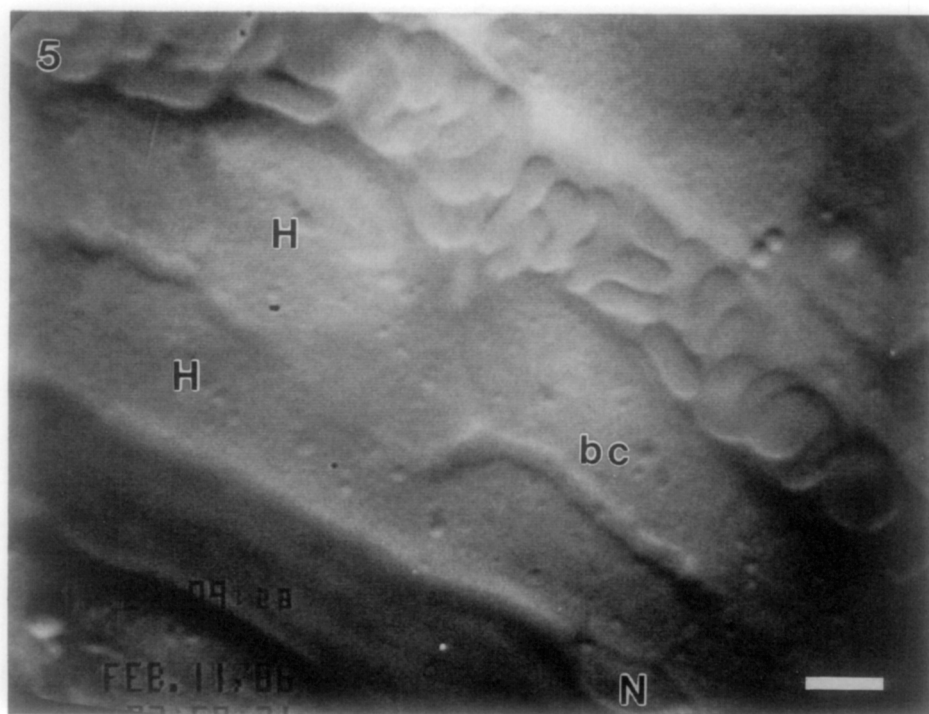


FIG. 5. *In vivo* microscopic view from normal mouse, showing adjacent sinusoids separated by two hepatocytes (H) with a bile canaliculus (bc) running between them. Sinusoid at bottom had rapid flow, whereas in sinusoid at top the flow was slower (due to partial blockage, transiently, with a white blood cell (not shown)) and individual RBC's may be distinguished. N, nucleus of sinusoidal lining cell. Bar = 5 μ m; $\times 2100$.

TABLE I
RBC VELOCITIES IN SINUSOIDS ADJACENT TO
LESIONS,^a AND IN NORMAL LIVERS

Measurement site	Velocity (μ m/sec: mean \pm SD; $N = 40-60$)
First (adjacent) sinusoid	17.4 \pm 6.7*
Second sinusoid	33.9 \pm 8.7*
Third sinusoid	66.6 \pm 27.3**
Normal liver	69.2 \pm 30.6

^a These sinusoids were aligned with the periphery of individual lesions. RBC velocities were measured in consecutive sinusoids, beginning with the most proximal (i.e., first) sinusoid with visible flow and moving outward from the lesions.

* Significantly different from mean velocity in normal liver ($P < 0.0005$).

** Not significantly different from mean velocity in normal liver ($P > 0.05$).

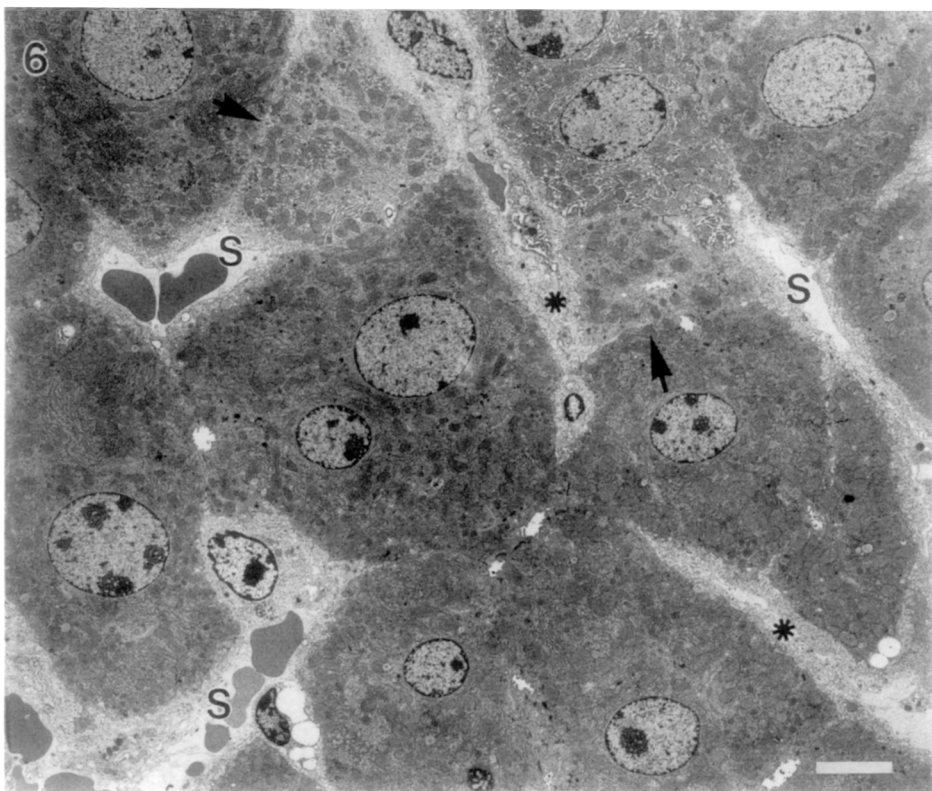


FIG. 6. Transmission electron micrograph of liver of MHV-3-infected mouse (36 hr postinfection). Some sinusoidal lumens are blocked by blood cells and debris (*), while other sinusoids (S) appear to be patent. Two hepatocytes which border a blocked sinusoid have a pale, vacuolated appearance (→). Bar = 5 μm ; $\times 2050$.

filling the lumen, with no plasma spaces evident. Kupffer cells were usually visible in these vessels, and swollen microvilli from the hepatocytes extended far into the lumen. The convex surfaces of some hepatocytes and their pale vacuolated cytoplasm suggested that these cells were swollen; in fact, sometimes hepatocytes were seen bulging into the lumen, blocking it completely. Blood cells of all types were present in the blocked sinusoids, presumably being trapped there.

No other quantitative data are available, to our knowledge, on RBC velocities in liver sinusoids of mice. However, we were surprised to find that our values in normal mice [$0.07 \text{ mm/s} \pm 0.03$ (SD)] were substantially lower than values reported for sinusoids of rat [$0.25 \text{ mm/sec} \pm 0.003$ (SE): Koo and Liang, 1979; $0.43 \text{ mm/s} \pm 0.10$ (SD): Unger and Reilly, 1986]. The difference in RBC velocities could not be explained on the basis of anesthetic or body temperature, since sodium pentobarbital anesthesia was used in all the foregoing experiments, and all animals were maintained at a core temperature of 37° . We were uncertain whether the results represented a difference between species or between methods of measurement (video flying-spot versus dual-window densitometric method). For this reason, we carried out RBC velocity measurements in liver sinusoids

of two normal rats (Wistar) and obtained a mean value of $0.18 \text{ mm/sec} \pm 0.13 \text{ (SD)}$ ($n = 45$). This is comparable to the value of 0.25 mm/sec found by Koo and Liang (1979). The higher value (0.43 mm/sec) obtained by Unger and Reilly (1986) was measured within the terminal portal venule at the inlet to sinusoids and would be expected to be somewhat greater than the velocity within the sinusoids themselves (where the present measurements and those of Koo and Liang were made). From recent data on RBC velocity within liver sinusoids in rat (Koo, 1987), obtained by the flying spot technique instead of the dual-window densitometric method, an overall mean velocity of $0.15 \text{ mm/sec} \pm 0.09 \text{ (SD)}$ ($n = 261$) was calculated (Koo, personal communication). The mean value we found in rat is in good agreement with these data. This lends support to the view that the difference we found in mean RBC velocities between mouse and rat represents a species difference. However, this does not appear to be due to a larger caliber of sinusoids in rat than in mouse, for the mean diameter we obtained in mouse [$6.2 \mu\text{m} \pm 1.8 \text{ (SD)}$; $n = 48$] is similar to the values obtained in rat [portal sinusoids, $5.9 \mu\text{m} \pm 0.17 \text{ (SE)}$, $n = 545$; central sinusoids, $7.1 \mu\text{m} \pm 0.29 \text{ (SE)}$, $n = 498$] by Wisse *et al.* (1985).

The present results show that the lesions in liver parenchyma of MHV-3-infected mice are focal in origin, contrary to the classical view of hepatitis as a diffuse necrosis. These lesions are most often found near terminal portal venules (Levy *et al.*, 1983; McPhee *et al.*, 1985), locations at which Kupffer cells are found in greatest abundance, as demonstrated by the uptake of particulate material (e.g., India ink). Pereira *et al.* (1984) have shown that destruction of sinusoidal lining cells (endothelial and Kupffer cells) by a frog virus (FV-3) can render the resistant A/J strain of mice susceptible to MHV-3. This suggests that infection of, or damage to, the sinusoidal lining cells may be the source of the procoagulant activity known to be released (Dindzans *et al.*, 1985; Maier and Hahnel, 1984; Geczy, 1984) with subsequent activation of the coagulation cascade. Furthermore, the release from macrophages of oxyradicals (and/or other cellular factors) which may be important mediators initiating hepatocellular membrane damage is currently under investigation (MacPhee and Keown, manuscript in preparation). Such damage could lead ultimately to cellular edema and necrosis, microthrombus formation, and blockage of sinusoids in the local area. This work adds to the evidence that sinusoidal lining cells are of crucial importance in the process of injury. The predominantly spherical shape of the lesions, observed both in microcorrosion casts and *in vivo*, suggests that progress of the injury may be by cell to cell spread, leading to gradually increasing necrosis in all directions.

ACKNOWLEDGMENTS

We thank Mrs. Barbara Anderson for typing the manuscript. The research was supported by a grant to A.C.G. from the Medical Research Council of Canada.

REFERENCES

- BLOCH, E. H., WARREN, K. S., AND ROSENTHAL, M. S. (1975). *In vivo* microscopic observations of the pathogenesis of acute mouse viral hepatitis. *Brit. J. Exp. Pathol.* **56**, 256-264.

- DINDZANS, V. J., MACPHEE, P. J., FUNG, L. S., LEIBOWITZ, J. L., AND LEVY, G. A. (1985). The immune response to mouse hepatitis virus: Expression of monocyte procoagulant activity and plasminogen activator during infection in vivo. *J. Immunol.* **135**, 4189-4197.
- GECZY, C. L. (1984). The role of lymphokines in delayed-type hypersensitivity reactions. *Springer Semin. Immunopathol.* **7**, 321-346.
- KOO, A. (1987). Nervous control of the hepatic microcirculation. In "Microcirculation—An Update" (M. Tsuchiya, M. Asano, Y. Mishima, and M. Oda, Eds), Vol. 2, pp. 335-338. Elsevier, Amsterdam.
- KOO, A., AND LIANG, I. Y. S. (1979). Microvascular filling pattern in rat liver sinusoids during vagal stimulation. *J. Physiol. (London)* **295**, 191-199.
- LE PROVOST, C., VIRELIZIER, J. L., AND DUPUY, J. M. (1975). Immunopathology of MHV-3 infection. III. Clinical and virologic observations of a persistent viral infection. *J. Immunol.* **115**, 640-643.
- LEVY, G. A., MACPHEE, P. J., FUNG, L. S., FISHER, M. M., AND RAPPAPORT, A. M. (1983). The effect of mouse hepatitis virus infection on the microcirculation of the liver. *Hepatology*, **3**, 964-973.
- MACDONALD, I. C., RAGAN, D. M., SCHMIDT, E. E., AND GROOM, A. C. (1987). Kinetics of red blood cell passage through interendothelial slits into venous sinuses in rat spleen, analyzed by *in vivo* microscopy. *Microvasc. Res.* **33**, 118-134.
- MACPHEE, P. J., DINDZANS, V. J., FUNG, L. S., AND LEVY, G. A. (1985). Acute and chronic changes in the microcirculation of the liver in inbred strains of mice following infection with mouse hepatitis virus type 3. *Hepatology* **5**, 649-660.
- MAIER, R. V., AND HAHNEL, G. S. (1984). Microthrombosis during endotoxemia: Potential role of hepatic versus alveolar macrophages. *J. Surg. Res.* **36**, 362-370.
- NOPANITAYA, W., AGHAJANIAN, J. G., AND GRAY, L. D. (1979). An improved plastic mixture for corrosion casting of the gastrointestinal microvascular system. In "Scanning Electron Microscopy/III," pp. 751-755. SEM, Inc. O'Hare, IL.
- PEREIRA, C. A., STEFFAN, A. M., AND KIRN, A. (1984). Kupffer and endothelial liver cell damage renders A/J mice susceptible to mouse hepatitis virus type 3. *Virus Res.* **1**, 557-563.
- TYML, K., AND ELLIS, C. G. (1982). Evaluation of the flying spot technique as a television method for measuring red cell velocity in microvessels. *Int. J. Microcirc. Clin. Exp.* **1**, 145-155.
- UNGER, L. S., AND REILLY, F. D. (1986). Hepatic microvascular regulatory mechanisms. VII. Effects of endoportally-infused endotoxin on microcirculation and mast cells in rats. *Microcirc. Endothelium Lymphatics* **3**, 47-74.
- WISSE, E., DE ZANGER, R. B., CHARELS, K., VAN DER SMISSSEN, P., AND MCCUSKEY, R. S. (1985). The liver sieve: Considerations concerning the structure and function of endothelial fenestrae, the sinusoidal wall and the space of Disse. *Hepatology* **5**, 683-692.